UCRL--93820

DE86 006701

EVALUATED RAYLEIGH INTEGRALS FOR PULSED PLANAR EXPANDING RING SOURCES

S. I. Warshaw

This paper was prepared for submittal to:
12th International Congress on Acoustics
Canadian Acoustical Association
Toronto, Canada
July 24 – 31, 1986

December 20, 1985

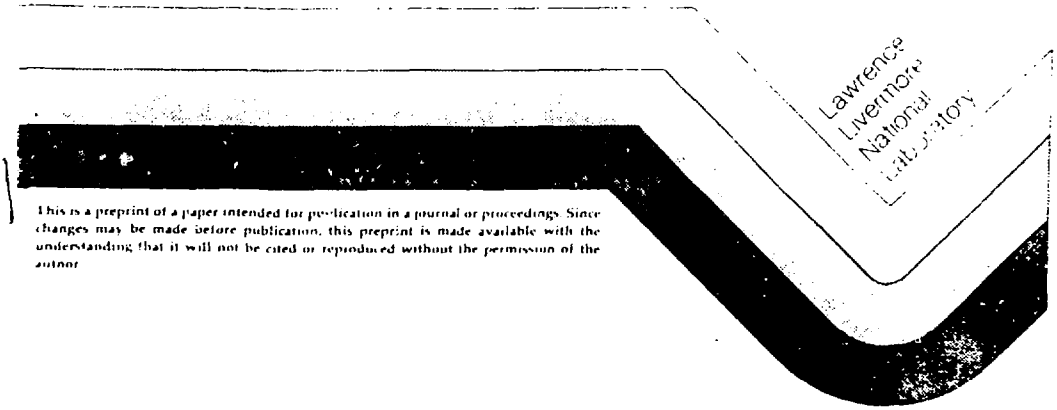

EVALUATED RAYLEIGH INTEGRALS FOR PULSED PLANAR EXPANDING RING SOURCES

S. I. Warshaw
Lawrence Livermore National Laboratory
Livermore, CA 94550

ABSTRACT

We have explicitly calculated time-domain analytic and semianalytic pressure fields acoustically radiated from expanding pulsed ring sources imbedded in a planar rigid baffle. The source functions are radially symmetric delta-function distributions whose amplitude and argument have simple functional dependencies on radius and time. Certain cases yield closed analytic results, while others result in elliptic integrals, which are evaluated to high accuracy by Gauss-Chebyshev and modified Gauss-Legendre quadrature. These results are of value for calibrating computer simulations and convolution procedures, and estimating fields from more complex planar radiators.

*Work performed under the auspices of the U.S. Department of Energy by the Lawrence Livermore National Laboratory under contract number W-7405-ENG-48.

The purpose of this paper is to present analytic and quasi-analytic time-domain representations for the impulsive pressure field radiated by a baffled circular membrane having a cylindrically symmetric normal surface acceleration history $a_n = f(r)\delta(t-g(r))$, where r is the radial surface distance from the center of the membrane, and to give examples resulting from simple forms for f(r) and g(r). Apart from pedagogic merits, these developments provide impulsive pressure field models well suited to a variety of applications, such as validation and calibration of other procedures used for calculating more complex sound fields, estimation of sound fields arising from similar but not identical sources, and parametric studies related to, e.g., distortions in source emission and ambient propagation conditions. The techniques we describe below can easily be programmed for very small portable digital computers.

The Basic Integral

We employ Rayleigh's integral to represent the acoustic pressure field produced by the source described above. The acoustic pressure history at an observation point off the source plane is [1]

$$p = \frac{\rho_o}{2\pi}\int a_n\left(t - \frac{R}{a_o}\right)\frac{d\sigma}{R}$$

where ρ_o and a_o are the ambient density and sound speed of the propagating medium, assumed constant, $d\sigma$ is the area element of the emitting source, and R is the slant distance from $d\sigma$ to the observation point.

We choose the coordinate system and geometry shown in Fig. 1, so that the observation point is c units above the source plane and b units from the surface normal through the source center. The source is taken to have finite radius a. We use the area element $d\sigma = \rho d\rho d\varphi = 2rdrdR/\sqrt{Q(r,R)}$, where $\rho^2 = R^2 - c^2$, and the cosine law $r^2 = b^2 + \rho^2 - 2\rho b\cos\varphi$ has been used to obtain $Q(r,R) = (2b\rho)^2 - (\rho^2 + b^2 - r^2)^2$. Thus the integral with which we shall be concerned is

$$I = \frac{2\pi p}{\rho_o} = 4\int_c^\infty\int_0^a \frac{r\, f(r)\, \delta\,(t - g(r) - R/a_o)\, drdR}{\sqrt{Q(r,R)}}$$

The additional factor of 2 arises from the radial symmetry of the source function. (Consideration of the "on-axis" (b=0) response leads to a different form of the integral, with analytic consequences. We omit this development here.)

We carry out the integration over r first, making use of properties of integrals with delta functions having function arguments and over finite limits. (See, for instance, [2]). The result is the following integral over R:

$$I = 4 \int_c^\infty \frac{r_o f(r_o)[H(a - r_o) - H(-r_o)]dR}{|g'(r_o)| \sqrt{Q(r_o,R)}}$$

where r_o is a zero of the argument of the retarded delta function. The Heaviside step functions further delimit the integration range, since r_o is necessarily a function of R (and t). If the delta function argument has more than one zero, then I splits into a sum of integrals, each associated with a different zero. We shall treat and give examples of integrals that result when $g(r) = r/v_s$ and $\sqrt{(r^2+z^2)}/v_s$, and when $f(r) = 1$ and $[1-(r/a)^n]^m$, where v_s, a, z, n, and m are constants.

Case I: $f = 1$, $g = r/v_s$

In this case $a_n = \delta(t - r/v_s)$ and describes an impulsive circular ring expanding uniformly outward with constant radial velocity v_s and unit amplitude. The zero of the corresponding retarded delta function argument is at $r_o = v_s t - \beta R$, where we have defined a source "Mach number" by $\beta = v_s/a_o$. The Heaviside functions limit R to $a_o(t - a/v_s) \le R \le a_o t$, and the radicand function becomes $Q(r_o,R) = 4b^2(R^2 - c^2) - [R^2 - c^2 + b^2 - (v_s t - \beta R)^2]^2$. This expression factors conveniently into a product of linear terms $-(\beta^2 - 1)^2 \prod (R - R_i)$, where the four R_i are given by $R_i = [\beta(v_s t \pm b) \pm \sqrt{((v_s t \pm b)^2 - (\beta^2 - 1)c^2)}] / (\beta^2 - 1)$. Then

$$I = \frac{4a_o\beta^2}{|\beta^2 - 1|} \int \frac{(a_o t - R)\,dR}{\sqrt{-(R-R_1)(R-R_2)(R-R_3)(R-R_4)}}$$

The limits of integration are further determined by requiring that the radical be real. It is therefore of interest to plot both the Heaviside function limits and the locus of the roots of $Q(r_o,R) = 0$ in the R–t plane, since for given t this readily indicates the integration range. Such a plot is shown in Fig. 2 for the specific case where $a_o = 1$, $v_s = 3$, $a = 7$, $b = 4$, and $c = 5$. Thus $\beta = 3$. The root loci are the intersecting hyperbolae $[(\beta + 1)R - (v_s t \pm b)][(\beta - 1)R - (v_s t \pm b)] = -c^2$ and the Heaviside function limits are the straight lines $r_o = 0$ and $r_o = a$. The shaded region represents values of R and t for which $Q(r_o,R) \ge 0$ and the Heaviside limit requirements are satisfied.

Several time marks of interest are clearly identifiable. The pulse history at the observation point starts at $t_F = (b + c\sqrt{(\beta^2-1)})/v_s$ corresponding to the Fermat path of minimum time for this problem; the slant distance is $R_F = \beta c/\sqrt{(\beta^2-1)}$. The onset of "edge cutoff" where the expanding ring is "seen" from the observation point to reach the near edge of the disk at r = a occurs at $t_i = a/v_s + R_i/a_o$. The pulse ends at $t_f = a/v_s + R_f/a_o$ when the expansion is "seen" to reach the far edge. Here, $R_{i,f} = \sqrt{(c^2 + (b \pm a)^2)}$ are the slant distances to these edges. The triple intersection of the two hyperbolae and the line $R = a_o t$, at $t_A = R_A/a_o$ where $R_A = \sqrt{(b^2+c^2)}$, corresponds to the propagation of the onset of the source motion at its center directly to the observation point. The boundary line $R = a_o(t - a/v_s)$ corresponds to $r_o = a$, and is the locus of (R,t) for which the signal of the expanding ring reaching the edge limit r = a propagates to the observation point. The time of minimum R ($R_m = c$), occurs at $t_m = b/v_s + c/a_o$.

We note that, in general, the time corresponding to signal reception from a particular surface point at r is $t = r/v_s + R/a_o$, while the extremes in slant range for a given r are $R = \sqrt{(c^2 + (b \pm r)^2)}$. On eliminating r from these two expressions we recover the condition $Q(r_o,R) = 0$. In this way we see that the two smallest roots R_i of $Q(r_o,R) = 0$ correspond to extreme propagation paths during the source motion.

From Fig. 2 we have three distinct classes of integration ranges, corresponding to the time intervals $[t_F, t_A]$, $[t_A, t_i]$ and $[t_i, t_f]$. These are, respectively, $[R_4, R_2]$, $[R_4, R_3]$ and $[a_o(t - a/v_s), R_3]$. In the first two classes both endpoints are integrand singularities, while in the third just the upper endpoint is singular. The integral is elliptic. However, the first two integration classes may be calculated by Gauss–Chebyshev quadrature of the first kind [3], which seems peculiarly suited to this form, while the third can be calculated by modified Gauss–Legendre quadrature [4]. We show, as curve "A" in Fig. 3, the pulse resulting from carrying out the indicated quadratures at each time point. The initial "Fermat jump" and later "edge cutoff" profiles are clearly evident.

The root loci and the integration range classes will change as the geometry and kinematics of the radiative problem change. If a is sufficiently small, the pulse will start at t_i instead of t_F, and the integration classes will now correspond to the time intervals $[t_i, t_A]$ and $[t_A, t_f]$, with respective integration ranges $[a_o(t - a/v_s), R_2]$ and $[a_o(t - a/v_s), R_3]$. Modified Gauss–Legendre quadrature is indicated for both. As b becomes progressively smaller, the hyperbolic loci will approach each other, and for $b < c/\sqrt{(\beta^2 - 1)}$ the Fermat point (R_F, t_F) will leave the "allowed" region. Then the start time of the pulse will always be t_A. Also, as v_s approaches and becomes less than a_o, the hyperbolic "arms" will open up; when $v_s = a_o$ the two "left asymptotes" will become parallel to the R–axis. Both will acquire negative slope for $v_s < a_o$. Then there is no "Fermat point," and the start time is likewise always t_A.

Analytic Solutions

For certain special values of t and for certain geometric and kinematic conditions, the integrals reduce to analytically solvable ones. In the particular case where $\beta > 1$ and $b > c/\sqrt{(\beta^2-1)}$, the pulse starts at t_F and analytic forms obtain for I at t_F and at t_A. In the limit as $t \to t_F$, R_2 and R_4 approach R_F, and I approaches $I(t_F) = 2\pi a_o \beta \sqrt{(1 - c/(b\gamma))}/\gamma$ where $\gamma = \sqrt{(\beta^2 - 1)}$, which is the "Fermat jump" amplitude at the leading edge. (In all other cases the starting amplitude is zero.) At $t = t_A$ the elliptic integral reduces to algebraic form, with the result that for small values of a, $I(t_A) = 4a_o\beta^2$ [arc sin $(\alpha + (\beta^2 - 1)\, a/(2b\beta^2)) -$ arc sin$(\alpha)]/(\beta^2 - 1)$, where $\alpha = \sqrt{(b^2 + c^2)} / (\beta b)$. For large values of a, the first arc sin term reduces to $\pi/2$.

For asymptotically large values of a and t, the pulse amplitude approaches the limiting value $I(\infty) = 2\pi a_o \beta/(\beta + 1) = 2\pi a_o v_s/(a_o + v_s)$. In the "hypersonic" case where $v_s \gg a_o$, the pulse approaches that obtained for the uniformly pulsed rigid piston, which is also analytic. (Compare, e.g., [5])

Case II: $f = 1$ $g = \sqrt{(r^2 + z^2)} / v_s$.

Here, $a_\eta = \delta(t - \sqrt{(r^2 + z^2)}/v_s)$ and describes an impulsive circular ring expanding outward as the trace of a uniformly expanding sphere intersecting the source plane. The source motion starts at $t = z/v_s$ and at later times has the ring radius $r = \sqrt{((v_s t)^2 - z^2)}$. Following the same general development as in Case I, the retarded argument of the delta function is $t - R/a_o - \sqrt{(r^2+z^2)}/v_s$, which is zero when $r = r_o = \sqrt{((v_s t - \beta R)^2 - z^2)}$, with β as before. This time $g'(r_o) = - r_o/(v_s(v_s t - \beta R))$. The nonvanishing of the Heaviside function combination implies the integration range given by $a_o(t - \sqrt{(a^2 + z^2)}/v_s) \le R \le a_o(t - z/v_s)$, where, as before, $r = a$ is the radial limit of the source motion.

The integral now (fortuitously) becomes identical in form to that of Case I, with the exception that now $Q(r_o,R) = 4b^2(R^2 - c^2) - (R^2 - c^2 + b^2 - (v_s t - \beta R)^2 + z^2)^2$. The requirement that $\sqrt{(Q(r_o,R))}$ be real, combined with the Heaviside function limits, again defines the actual limits of integration. This $Q(r_o,R)$ is not biquadratic in R, and the four roots of $Q(r_o,R) = 0$ are best obtained by a root-finding procedure such as Newtonian iteration. We readily obtain a picture of the root loci, however, by solving instead for t; the result is $t = R/a_o \pm \sqrt{[z^2 + (b \pm \sqrt{(R^2 - c^2)})^2]}/v_s$, where a different locus obtains for each of the four arrangements of the $\pm$ signs.

In Fig. 4, we plot the new root loci in the R – t plane, using the same values of a_o, v_s, a, b, and c as in Case I, and with z = 1. We see immediately that the hyperbolic forms have "separated", so to speak. The asymptotes for these loci are precisely the same as in Case I. The shaded region, as before, indicates the allowed values of R and t for the integration. As with Case I, the point pairs of the lower curve for given t correspond to extremes of propagation path during the source motion.

The discussion of the features of this plot, and the integration procedures, essentially follow that of Case I, but with some obvious differences. There is no longer a triple intersection as before; instead the line $R = a_o(t - z/v_s)$ is tangent to the lower curve at the time $t = t_A = z/v_s + R_A/a_o$, where $R_A = \sqrt{(b^2 + c^2)}$. This corresponds to propagation of the onset of the source from its center to the observation point. There is now always a minimum "Fermat time" t_F and "Fermat range" R_F at which the pulse begins, unless the source radial limit r = a is sufficiently small so that the pulse starts at t_i.

The resulting pulse that corresponds to the allowed region of integration is similar to that shown for Case I, and is not displayed here.

The "Sonic" Cases

Both Case I and Case II integrals reduce to arc sine functions when $v_s = a_o$, and therefore $\beta = 1$, for then $Q(r_o,R)$ becomes quadratic in R. Thus, for Case II the sonic result is in two parts. For $t_F < t < t_i$, $I = \pi a_o A (s^2 - b^2)^{-s/2}$, and for $t_i \le t \le t_f$ (the edge cutoff region) we have $I = a_o(s^2 - b^2)^{-s/2}$ [A arc cos ((A – C)/B) – $\sqrt{(B^2 - (A - C)^2)}$] where $s = a_o t$, $A = s(s^2 - b^2 - c^2 + z^2)$, $B = b\sqrt{((s^2 - b^2 - (c + z)^2)(s^2 - b^2 - (c - z)^2))}$, $C = 2(s^2 - b^2)\sqrt{(a^2 + z^2)}$, and $t_F = \sqrt{(b^2 + (c + z)^2)}/a_o$. The corresponding sonic result for Case I may be obtained simply by setting z = 0; then the pulse starts at $t_A = \sqrt{(b^2 + c^2)}/a_o$.

Response With Source Amplitude Variation

We consider $f(r) = (1 - (r/a)^n)^m$. Appending this radial variation to the Case I and II integrands presents no additional difficulties, because the root loci $Q(r_o,R) = 0$ and the integration limits are not thereby modified. With the appropriate r_o, we simply multiply the integrand function by $(1 - (r_o/a)^n)^m$, and carry out the indicated quadratures without change in procedure. As an example, we consider $a_n = (1 - (r/a)^n)^m \delta(t - r/v_s)$, with n = 8, m = 2, and all other parameters the same as case I. The result of the quadratures is shown as curve "B" in Fig. 3. This n,m combination produces only a mild "edge falloff" of the source amplitude, yet the effects produced are quite striking.

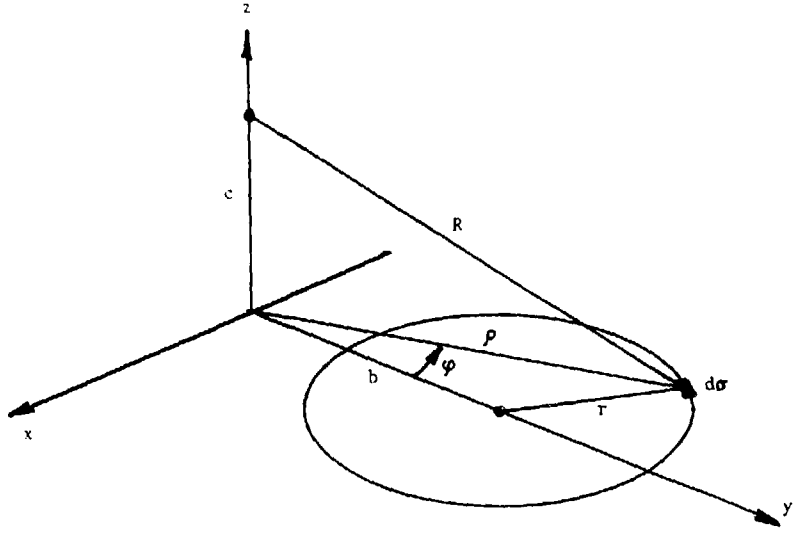

Figure 1. Geometry and coordinate system

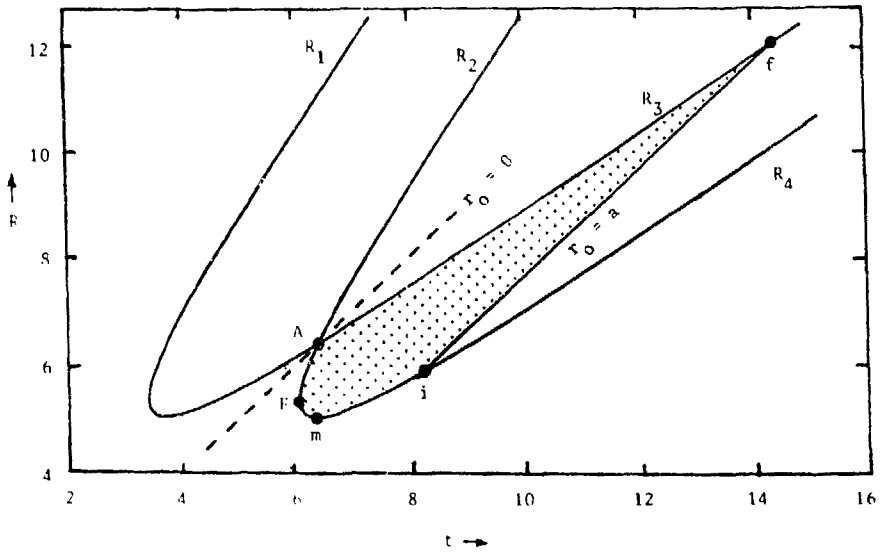

Figure 2. Root loci for Case I

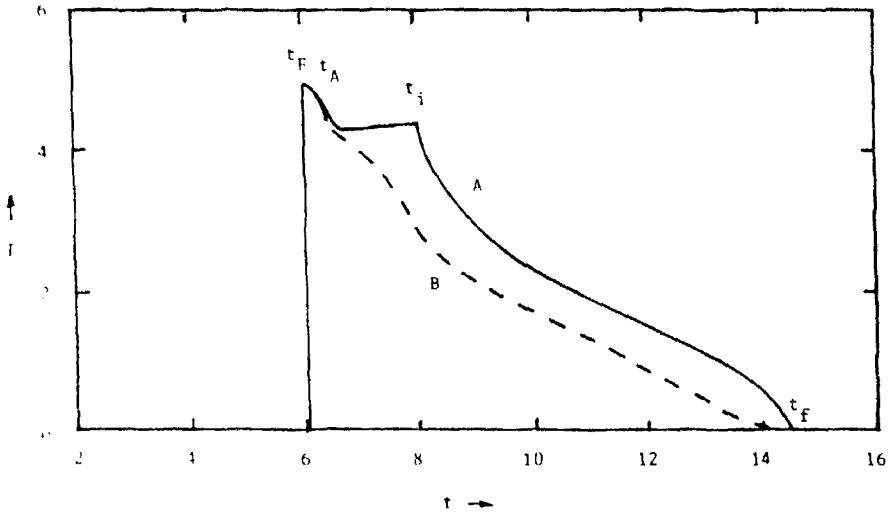

Figure 3. Pulse shapes for Case I

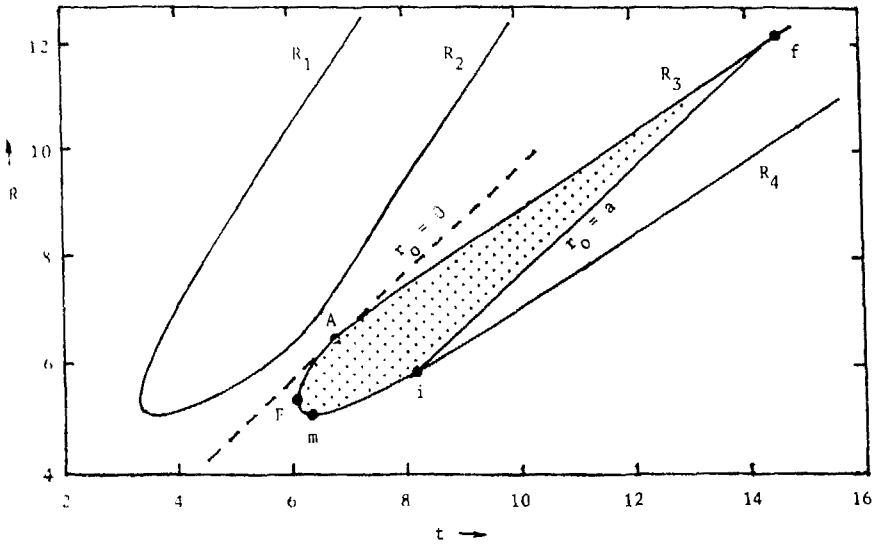

Figure 4. Root loci for Case II

REFERENCES

1. A. D. Pierce, Acoustics (McGraw-Hill, 1981), p. 214.

2. E. Zauderer, Partial Differential Equations of Applied Mathematics (Wiley, 1983), Sec. 7.2.

3. M. Abramowitz and I. A. Stegun, Handbook of Mathematical Functions (Dover, 1972), p. 889, Formula 25.4.39.

4. Ibid., Formula 25.4.37.

5. Pierce, ibid., pp. 227–231.